Available online at www.sciencedirect.com
ScienceDirect
Trans. Nonferrous Met. Soc. China 28(2018) 1397−1403
Transactions of Nonferrous Metals Society of China
www.tnmsc.cn

Enhanced cycling stability of Mg−F co-modified $LiNi_{0.6}Co_{0.2}Mn_{0.2-y}Mg_yO_{2-z}F_z$ for lithium-ion batteries

Qi-chao CHEN, Guan-jie YAN, Li-ming LUO, Fei CHEN, Tang-feng XIE, Shi-can DAI, Ming-liang YUAN

School of Minerals Processing and Bioengineering, Central South University, Changsha 410083, China

Received 13 March 2017; accepted 18 September 2017

Abstract: The layered $LiNi_{0.6}Co_{0.2}Mn_{0.2-y}Mg_yO_{2-z}F_z$ ($0\le y\le 0.12$, $0\le z\le 0.08$) cathode materials were synthesized by combining co-precipitation method and high temperature solid-state reaction, with the help of the ball milling, to investigate the effects of F−Mg doping on $LiNi_{0.6}Co_{0.2}Mn_{0.2}O_2$. Compared with previous studies, this doping treatment provides substantially improved electrochemical performance in terms of initial coulombic efficiency and cycle performance. The $LiNi_{0.6}Co_{0.2}Mn_{0.11}Mg_{0.09}O_{1.96}F_{0.04}$ electrode delivers an high capacity retention of 98.6% during the first cycle and a discharge capacity of 189.7 mA·h/g (2.8−4.4 V at 0.2*C*), with the capacity retention of 96.3% after 100 cycles. And electrochemical impedance spectroscopy(EIS) results show that Mg−F co-doping decreases the charge-transfer resistance and enhances the reaction kinetics, which is considered to be the major factor for higher rate performance. It is demonstrated that $LiNi_{0.6}Co_{0.2}Mn_{0.11}Mg_{0.09}O_{1.96}F_{0.04}$ is a promising cathode material for lithium-ion batteries for excellent electrochemical properties.

Key words: nickel-rich cathode material; F−Mg doping; high columbic efficiency; cycling stability

1 Introduction

With the continuous development of society, energy consumption has become a global problem, so there is drastically increased demand for new green energy [1]. As an energy storage and conversion device, the lithium-ion battery (LIB) shows many advantages, such as large energy density, high transform efficiency, little pollution and portability [2]. LIBs have been used in a broad range of applications, like cell phone, notebook, electric car and medical equipment [3]. Cathode material plays an important role in LIB, and the cathode material directly determines its performance.

Traditional research on cathode materials of LIB mainly concentrated on the transition metal oxides with layered structure such as $LiNiO_2$, $LiCoO_2$, $LiMnO_2$ and their derivatives. $LiCoO_2$ is one of the first commercial LIB cathode material, but its application is limited because of the scarce cobalt resources, high price and toxicity [4−6]. The difficult preparation and over charge security of $LiNiO_2$ seriously restrict its commercialization [7−9]. The layered $LiMnO_2$ has a high theoretical specific capacity (C_m) of 285 mA·h/g. However, its structure easily changes to the spinel structure during the charging and discharging process, resulting in the rapid decay of specific capacity [10−12]. Recently, intensive efforts have been directed towards the layered Li−Ni−Co−Mn−O (e.g. $LiNi_{0.5}Mn_{0.3}Co_{0.2}O_2$) composites for their high capacity, good cycling stability and security [13−18]. Among them, $LiNi_{0.6}Co_{0.2}Mn_{0.2}O_2$ [19,20] has been investigated as a promising cathode material. In order to increase the availability of cathode material in electric vehicles and other high-power devices, it is necessary to improve its electrochemical performance.

At present, researchers at home and abroad have improved the performance of materials by doping and coating [21−24]. So far, Mg has been used successfully to improve the cycling stability of cathode materials such as $LiNi_{1-x}Co_xO_2$ [25] and $LiLi_{0.2}Ni_{0.2}Mn_{0.6}O_2$ [26]. The improved performance is attributed to the enhanced conductivity and structural stability [25]. Fluorine substitution at the oxygen site has been reported to be effective for improving cycle life and rate performance of the cathode active materials for lithium-ion batteries [27,28]. By understanding the effect of F−Mg doping on the electrochemical performance of electrode materials,

Foundation item: Project (1114022-15) supported by the Major Science and Technology Research Projects of Guangxi Province, China
Corresponding author: Ming-liang YUAN; Tel/Fax: +86-731-88877209; E-mail: mlydoc@126.com
DOI: 10.1016/S1003-6326(18)64778-8

the rate and cycling properties of electrode materials can be improved effectively. Thus, F-doping can be widely applied in the cathode materials. In this work, $LiNi_{0.6}Co_{0.2}Mn_{0.2}O_2$ was prepared by a co-precipitation method, and material was doped with Mg and F elements. The effects of doping elements and doping ratio on electrochemical were investigated.

2 Experimental

2.1 Preparation of cathode materials

The precursor $Ni_{0.6}Co_{0.2}Mn_{0.2-y}Mg_y(OH)_2$ was prepared by the co-precipitation. Nickel sulfate ($NiSO_4·6H_2O$), cobalt sulfate ($CoSO_4·7H_2O$), manganese sulfate ($MnSO_4·H_2O$) and magnesium sulfate ($MgSO_4$) were dissolved in deionized water in a certain molar ratio of Co:Ni:(Mn+Mg)=2:6:2 with different doping amounts of Mg (0, 3%, 6%, 9% and 12%). Then, sodium hydroxide (NaOH) solution was added into the mixture with 1:1.2 (*V*/*V*) of NH_3/H_2O to obtain a solution with the pH value of about 11. It was subsequently stirred under 1000 r/min at 50 °C for 12 h to react, then rested for 10 h. After washing, it was dried at 120 °C for 8 h to obtain precursor $Ni_{0.6}Co_{0.2}Mn_{0.2-y}Mg_y(OH)_2$. Then, the dried precursor was ground with Li_2CO_3 and LiF with a certain molar ratio of $(OH^-+F^-):Li^+=1:1$, when the doping amounts of F^- were 0, 2%, 4%, 6% and 8%, respectively, to obtain different mixtures. The powders were subsequently annealed at 900 °C in air for 20 h followed by a natural cooling step to obtain $LiNi_{0.6}Co_{0.2}Mn_{0.2-y}Mg_yO_{2-z}F_z$ powders.

2.2 Physical characterization

The powder X-ray diffraction (XRD, DX−2700) measurement, using Cu K_α radiation (λ=0.154 nm) in the range of 10°−80° (2θ) with a step width of 0.02°, was used to identify the crystalline phase. The particle size and morphology of the $LiNi_{0.6}Co_{0.2}Mn_{0.2-y}Mg_yO_{2-z}F_z$ powders were observed by a scanning electron microscope (JSM−6360LV) with an accelerating voltage of 20 kV.

2.3 Electrochemical properties evaluation

The electrochemical characterization was performed using CR2025 coin-type cell by GAMRY Reference 600 electrochemical workstation. For positive electrode fabrication, the prepared powders were mixed with 10% (mass fraction) of carbon black and 10% (mass fraction) of polyvi-nylidene fluoride (PVDF) in N-methyl pyrrolidinone (NMP) until slurry was obtained. And then, the blended slurries were pasted onto an aluminum current collector, and the electrode was dried at 120 °C for 10 h in vacuum. The test cell consisted of the positive electrode and lithium foil (negative electrode) separated by a porous polypropylene (PP) film, with 1 mol/L $LiPF_6$ in EC:EMC:DMC (1:1:1 in volume) as the electrolyte. The assembly of the cells was carried out in a dry Ar-filled glove box. The cells were charged and discharged over a voltage range of 2.8 to 4.4 V versus Li/Li^+ electrode at room temperature. Cyclic voltammograms were tested in the three-electrode system using metallic foils as both counter and reference electrodes at a scanning rate of 0.1 mV/s in the voltage range of 3.0−4.8 V. EIS experiments were performed with a 10 mV voltage magnitude in the range of 0.01 Hz−100 kHz.

3 Results and discussion

3.1 XRD and chemical components analysis

Figure 1 shows the XRD patterns of prepared $LiNi_{0.6}Co_{0.2}Mn_{0.2-y}Mg_yO_{2-z}F_z$ (y=0.09, z=0.04). As shown in Fig. 1, all the reflection peaks indicate that the samples have standard α-$NaFeO_2$-type layered structure with the space group $R\bar{3}m$ [29], expect for the super lattice ordering between 20° and 25°. Many researches point out that these super lattice peaks are caused by the $LiMn_6$ cation ordering which exists in the transition metal layers of Li_2MnO_3 [30]. Another observation in the XRD patterns is the clear splitting of the (006)/(102) and (108)/(110) peaks, indicating that the materials have a well-organized layered structure [31]. No peak of any impurity phase is detected in the XRD patterns of Mg−F co-doped samples, indicating that the small amount of Mg−F co-doping has no impact on the significant structure of the cathode material.

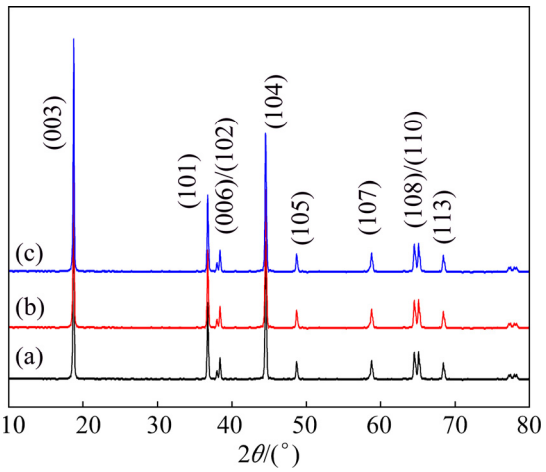

Fig. 1 XRD patterns of pristine and Mg-, F-doped cathode materials: (a) $LiNi_{0.6}Co_{0.2}Mn_{0.2}O_2$; (b) $LiNi_{0.6}Co_{0.2}Mn_{0.2}O_{1.96}F_{0.04}$; (c) $LiNi_{0.6}Co_{0.2}Mn_{0.11}Mg_{0.09}O_{1.96}F_{0.04}$

The lattice parameters of all samples are calculated and summarized in Table 1. The *c*/*a* ratios of all samples

are greater than 4.9, which is well known for a material with layered characteristic [32,33]. As the ionic radius of Mg^{2+} (0.72 Å) is larger than that of Ni^{2+} (0.69 Å), Mn^{4+} (0.53 Å) and Co^{3+} (0.54 Å), the lattice parameter *c* indicates that interlayer spacing increases after doping. The process of Li^+ intercalation/deintercalation will be facilitated by the enlargement of *c* value.

The intensity ratio (*R*) of *I*(003)/*I*(104) is sensitive to the cation distribution in the lattice and the degree of cation mixing of materials [34]. When the *R* value is higher, the degree of cation mixing is lower. It is reported that the undesirable cation mixing would appear when *R* is smaller than 1.2 [32,33]. The *R* value of all samples is larger than 1.2, which implies that the cation mixing is very weak for all samples. The value of *R* increases after doping. It can be expected that the undoped samples are more prone to cation mixing than the Mg−F co-doped ones. This is because the Mg element is more likely to occupy the Li site because of a small difference in size between Mg^{2+} (0.72 Å) and Li^+ (0.76 Å), in contrast with other cations: Mn^{4+} (0.53 Å), Co^{3+} (0.54 Å) and Ni^{2+} (0.69 Å). The cation mixing of Li/Mg exchange will restrain that of Li/Ni exchange, the latter might induce structural collapse by the radius changes of nickel ions (Ni^{2+}/Ni^{3+}/Ni^{4+}) during charge and discharge process [35]. In addition, the F^- doping can also improve the crystallinity of materials. Because the electronegativity of F^- is stronger than that of O^{2-}, the doping of F can hinder the transformation of Ni^{4+} to Ni^{2+}, which can also restrain the cation mixing (Li/Ni exchange).

Table 2 lists the chemical composition of prepared $LiNi_{0.6}Co_{0.2}Mn_{0.2-y}Mg_yO_{2-z}F_z$ (y=0.09, z=0.04). As we known, Li will loss at the temperature of 900 °C. It can be seen that, by increasing the content of lithium source, the lithium content of positive electrode material in a reasonable range, and theoretical molar ratio of positive electrode material are obtained.

3.2 SEM of synthesized $LiNi_{0.6}Co_{0.2}Mn_{0.2-y}Mg_yO_{1.96}F_{0.04}$ samples

The microstructures of $LiNi_{0.6}Co_{0.2}Mn_{0.2-y}Mg_yO_{1.96}F_{0.04}$ (y=0, 0.06, 0.09, 0.12) powders are illustrated in Fig. 2, where a small change in the morphology of particles by Mg doping can be identified. For the samples with y=0, the particle size is about 0.5 μm. With increasing amount of Mg^{2+} doped, the particle size of the prepared powders slightly decreases. It could be noticed that y=0.09 exhibits the relative uniform particle size, there are some primary particles and larger secondary ones while y=0, 0.06, 0.12.

3.3 Electrochemical performance

To investigate the effect of F−Mg doping on the electrochemical properties of cathode materials, the charge−discharge tests were carried out at the rate of 0.2*C* in the voltage range of 2.8−4.4 V at room temperature. As seen in Fig. 3, the specific capacities of the first charging and discharging test of three doped materials were compared. The initial charge capacities of $LiNi_{0.6}Co_{0.2}Mn_{0.2}O_2$, $LiNi_{0.6}Co_{0.2}Mn_{0.2}O_{1.96}F_{0.04}$, and $LiNi_{0.6}Co_{0.2}Mn_{0.11}Mg_{0.09}O_{1.96}F_{0.04}$ are 201.5, 188.9 and 192.4 mA·h/g, and the discharge capacities are 180.3, 181.6 and 189.7 mA·h/g, respectively. The correspon-ding coulombic efficiencies are 89.5%, 96.1% and 98.6%, respectively. It is clearly seen that the electrode reaction reversibility is enhanced considerably when the pristine cathode powder is doped by F−Mg. The F doping leads to deceasing the expansion rate of the crystal lattice *c*, which improves the stability of the layered structure, so that a small amount of F-doped samples present excellent cycle properties. Although Mg^{2+} has no electrochemical activity, it plays a role in supporting inter-layers when the crystal lattice distortion is caused by the change of valence state of nickel during the charging−discharging process. Accordingly, the F−Mg doping is beneficial to the improvement of coulombic efficiency.

Table 1 Lattice parameters of pristine and F-, Mg-doped cathode materials

Sample	*a*/Å	*c*/Å	*c*/*a*	*I*(003)/ *I*(104)
$LiNi_{0.6}Co_{0.2}Mn_{0.2}O_2$	2.8663	14.2370	4.967	1.454
$LiNi_{0.6}Co_{0.2}Mn_{0.2}O_{1.96}F_{0.04}$	2.8673	14.2476	4.969	1.524
$LiNi_{0.6}Co_{0.2}Mn_{0.11}Mg_{0.09}O_{1.96}F_{0.04}$	2.8643	14.2298	4.968	1.598

Table 2 Chemical composition of positive electrode materials

Sample	Theoretical amount/mol				Actual amount/mol			
	Li	Ni	Co	Mn	Li	Ni	Co	Mn
$LiNi_{0.6}Co_{0.2}Mn_{0.2}O_2$	1.000	0.600	0.200	0.200	0.998	0.598	0.201	0.199
$LiNi_{0.6}Co_{0.2}Mn_{0.2}O_{1.96}F_{0.04}$	1.000	0.600	0.200	0.200	0.999	0.597	0.202	0.201
$LiNi_{0.6}Co_{0.2}Mn_{0.11}Mg_{0.09}O_{1.96}F_{0.04}$	1.000	0.600	0.200	0.110	0.997	0.599	0.199	0.112

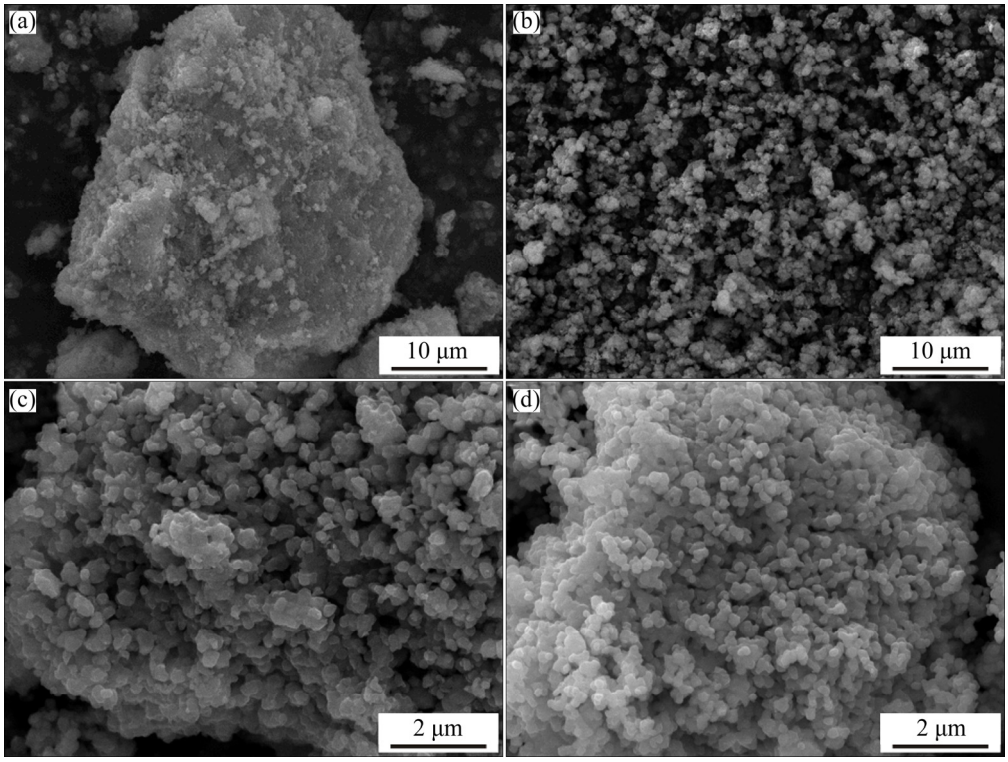

Fig. 2 SEM images of $LiNi_{0.6}Co_{0.2}Mn_{0.2-y}Mg_yO_{1.96}F_{0.04}$ samples calcined at 900 °C for 20 h: (a) y=0; (b) y=0.06; (c) y=0.09; (d) y=0.12

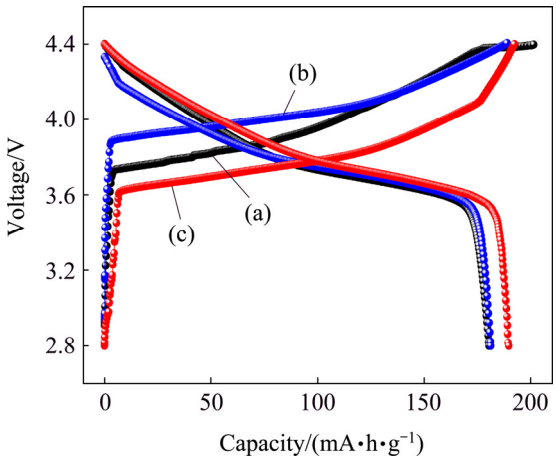

Fig. 3 Initial charge−discharge curves of $LiNi_{0.6}Co_{0.2}Mn_{0.2-y}Mg_yO_{2-z}F_z$ samples: (a) $LiNi_{0.6}Co_{0.2}Mn_{0.2}O_2$; (b) $LiNi_{0.6}Co_{0.2}Mn_{0.2}O_{1.96}F_{0.04}$; (c) $LiNi_{0.6}Co_{0.2}Mn_{0.11}Mg_{0.09}O_{1.96}F_{0.04}$

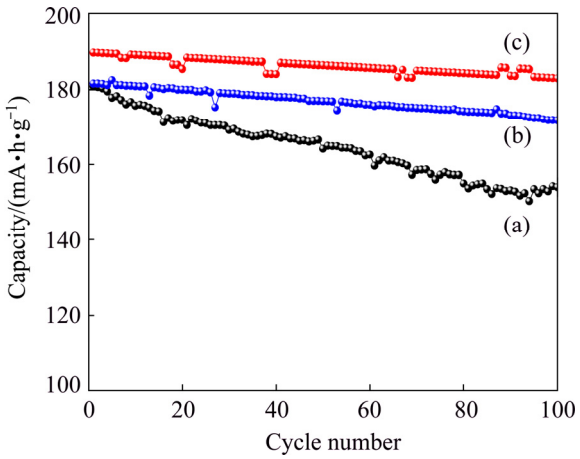

Fig. 4 Cycling performance of $LiNi_{0.6}Co_{0.2}Mn_{0.2-y}Mg_yO_{2-z}F_z$ samples at 0.2C discharge rate: (a) $LiNi_{0.6}Co_{0.2}Mn_{0.2}O_2$; (b) $LiNi_{0.6}Co_{0.2}Mn_{0.2}O_{1.96}F_{0.04}$; (c) $LiNi_{0.6}Co_{0.2}Mn_{0.11}Mg_{0.09}O_{1.96}F_{0.04}$

Figure 4 compares the cycling performance of $LiNi_{0.6}Co_{0.2}Mn_{0.2}O_2$, $LiNi_{0.6}Co_{0.2}Mn_{0.2}O_{1.96}F_{0.04}$, $LiNi_{0.6}Co_{0.2}Mn_{0.11}Mg_{0.09}O_{1.96}F_{0.04}$ samples. The electrochemical cycling performance was evaluated in the $Li/LiNi_{0.6}Co_{0.2}Mn_{0.2-y}Mg_yO_{2-z}F_z$ cell configuration at room temperature in the voltage range of 2.8−4.4 V at 0.2C charge rate. As seen in Fig. 4, the specific capacities for $LiNi_{0.6}Co_{0.2}Mn_{0.2-y}Mg_yO_{2-z}F_z$ (y=0.09, z=0.04) samples at 0.2C discharge rates are higher than that for pristine $LiNi_{0.6}Co_{0.2}Mn_{0.2}O_2$. $LiNi_{0.6}Co_{0.2}Mn_{0.11}Mg_{0.09}O_{1.96}F_{0.04}$ demonstrates remarkably improving the specific capacity and cycling performance. From Fig. 4(a), at 0.2C discharge rate, the specific capacity of un-doped $LiNi_{0.6}Co_{0.2}Mn_{0.2}O_2$ is only 155.4 mA·h/g after 100 cycles, with capacity retention of 86.2%. Whereas, these values of $LiNi_{0.6}Co_{0.2}Mn_{0.2}O_{1.96}F_{0.04}$, $LiNi_{0.6}Co_{0.2}Mn_{0.11}Mg_{0.09}O_{1.96}F_{0.04}$ are 171.9 and 182.6 mA·h/g, with capacity retentions of 94.7% and 96.3%, respectively. This result is expected because of the higher electronic

conductivity of Mg−F-substituted $LiNi_{0.6}Co_{0.2}Mn_{0.2}O_2$ compared with the pristine samples. These results indicate that Mg−F substitution can improve the electronic conductivity, diffusion of Li^+ and cycling stability. Indeed, the sample of $LiNi_{0.6}Co_{0.2}Mn_{0.11}Mg_{0.09}O_{1.96}F_{0.04}$ shows the best electrochemical performance.

Figure 5 shows the alternating current (AC) impedance plots of $LiNi_{0.6}Co_{0.2}Mn_{0.2}O_{1.96}F_{0.04}$ and $LiNi_{0.6}Co_{0.2}Mn_{0.2}O_2$ electrodes at about 3 V. A semicircle was observed to center on the real axis in the high frequency range. In the low frequency range, a straight line with an angle of 45° to the real axis corresponds to the Warburg impedance. The high frequency semicircle is related to the charge-transfer resistance (R_{ct}) and the double-layer capacitance. The low frequency tails resulted from the diffusion of Li^+ in the bulk active mass. In the case of $LiNi_{0.6}Co_{0.2}Mn_{0.2}O_2$, the diameter of the semicircle significantly depends on the potential during charging, indicating that the film formation process is dependent on the Li^+ content. On the other hand, the charge-transfer resistance, shows a greater dependence on the lithium insertion and extraction levels. In the highly charged states, the sample was found to give low R_{ct} values. Comparing the diameters of the semicircle of the above two systems, it can be found that $LiNi_{0.6}Co_{0.2}Mn_{0.2}O_{1.96}F_{0.04}$ showed lower R_{ct} value than $LiNi_{0.6}Co_{0.2}Mn_{0.2}O_2$, indicating that the F-doping may cause some defects in the $LiNi_{0.6}Co_{0.2}Mn_{0.2}O_2$ system, which increases the electronic conductivity and improves the Li^+ kinetic behavior.

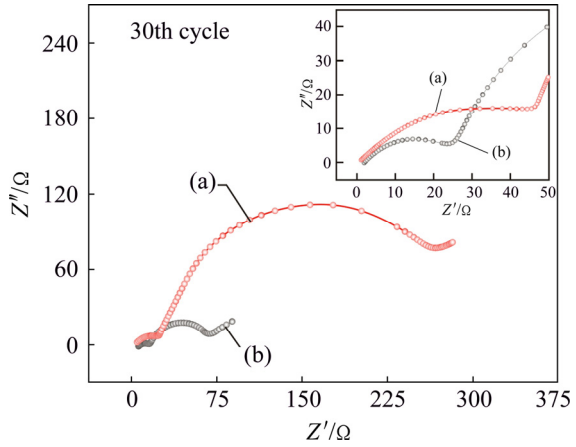

Fig. 5 Nyquist plots of $LiNi_{0.6}Co_{0.2}Mn_{0.2}O_2$ (a) and $LiNi_{0.6}Co_{0.2}Mn_{0.2}O_{1.96}F_{0.04}$ (b)

Figure 6 shows the AC impedance plots of $LiNi_{0.6}Co_{0.2}Mn_{0.2}O_{1.96}F_{0.04}$ and $LiNi_{0.6}Co_{0.2}Mn_{0.11}Mg_{0.09}O_{1.96}F_{0.04}$. This result is well in accordance with the rate capability. The decreased resistance can be attributed to the enhanced conductivity by Mg−F doping. All in all, the doped samples reveal much lower values compared with the ones for pristine sample, which can be ascribed to three reasons: 1) the doping particles possess more 3D channels for Li diffusion; 2) the doping treatment also leads to a collapse of Ni segregation which could suppress negative effects on fast transportation of Li between terminated surfaces and the bulk; 3) the doping particle may provide better surface conductivity leading to significantly reduced R_{ct}. In fact, such observations on EIS are consistent with the results obtained from electrochemical testing.

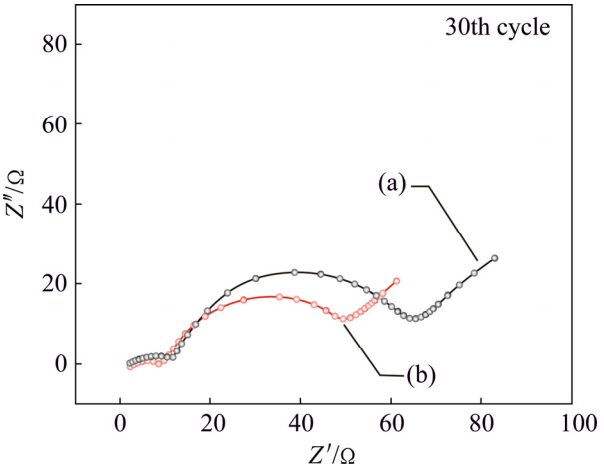

Fig. 6 Nyquist plots of $LiNi_{0.6}Co_{0.2}Mn_{0.2}O_{1.96}F_{0.04}$ (a) and $LiNi_{0.6}Co_{0.2}Mn_{0.11}Mg_{0.09}O_{1.96}F_{0.04}$ (b)

Cyclic voltammetry (CV) measurements were carried out to compare electrochemical behaviors of the electrodes at a sweep rate of 0.1 mV/s. The peak potentials and peak current in the CV curve represent the electrochemical characteristics of the materials and reveal the phase transitions that occur during detercalation/intercalation of Li ions. As shown in Fig. 7, all curves of the electrodes showed a similar profile. The appearance of only one couple of peaks in the $LiNi_{0.6}Co_{0.2}Mn_{0.2-y}Mg_yO_{2-z}F_z$/Li cell between 3.2 and 4.6 V means that no structural transitions exist from hexagonal to monoclinic, which is believed to limit the reversible charge/discharge capacity in $LiCoO_2$. The oxidation peak of $LiNi_{0.6}Co_{0.2}Mn_{0.2}O_2$ was observed at around 4.05 V, coupled with the reduction peak at 3.67 V; the oxidation peak of $LiNi_{0.6}Co_{0.2}Mn_{0.2}O_{1.96}F_{0.04}$ was observed at around 4.03 V, coupled with the reduction peak at 3.79 V. In the case of $LiNi_{0.6}Co_{0.2}Mn_{0.11}Mg_{0.09}O_{1.96}F_{0.04}$ electrode, the oxidation peaks shifted down to 3.98 V, while the reduced peaks shifted up to 3.81 V. Namely, the potential difference for the redox couples of $LiNi_{0.6}Co_{0.2}Mn_{0.11}Mg_{0.09}O_{1.96}F_{0.04}$ was reduced, which indicates that the reversibility of the electrode reaction could be enhanced by Mg−F co-doping.

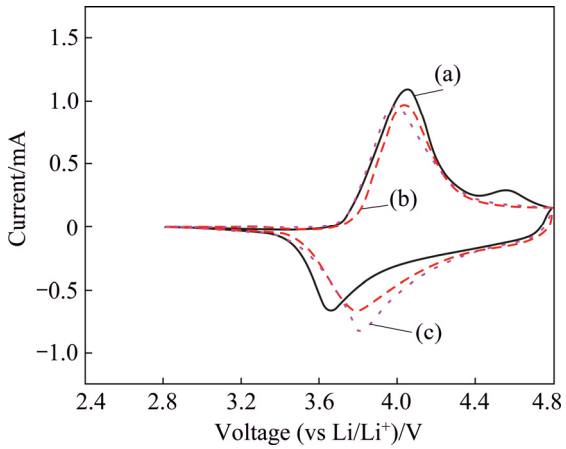

Fig. 7 CV curves of $LiNi_{0.6}Co_{0.2}Mn_{0.2-y}Mg_yO_{2-z}F_z$ samples: (a) $LiNi_{0.6}Co_{0.2}Mn_{0.2}O_2$; (b) $LiNi_{0.6}Co_{0.2}Mn_{0.2}O_{1.96}F_{0.04}$; (c) $LiNi_{0.6}Co_{0.2}Mn_{0.11}Mg_{0.09}O_{1.96}F_{0.04}$

4 Conclusions

1) XRD results of Mg−F-co-doped $LiNi_{0.6}Co_{0.2}Mn_{0.2-y}Mg_yO_{2-z}F_z$ powders show that they exhibit similar XRD patterns as those of pristine cathode materials.

2) Electrochemical charge/discharge measurements in lithium-ion cells indicate that the Mg−F-co-doped samples exhibit high discharge capacity and superior rate capability. The F−Mg-doped $LiNi_{0.6}Co_{0.2}Mn_{0.2}O_2$ has better electrochemical performance than the bare $LiNi_{0.6}Co_{0.2}Mn_{0.2}O_2$. At 0.2*C* rate, the initial coulombic efficiency of the $LiNi_{0.6}Co_{0.2}Mn_{0.2}O_2$ is improved from 89.5 % to 98.6 % by F−Mg co-doping. And the capacity retention is improved from 86.2% to 96.3 % after 100 cycles at 0.2*C* rate.

3) EIS results show that Mg−F doping decreases the charge-transfer resistance and enhances the reaction kinetics, which is considered to be the major factor for high rate performance. In brief, $LiNi_{0.6}Co_{0.2}Mn_{0.11}Mg_{0.09}O_{1.96}F_{0.04}$ is characterized to be a promising cathode material for lithium ion batteries.

References

[1] DUNN B, KAMATH H, TARASCON J M. Electrical energy storage for the grid: A battery of choices [J]. Science, 2011, 334(6058): 928−935.

[2] WU H B, CHEN J S, HNG H H, LOU X W. Nanostructured metal oxide-based materials as advanced anodes for lithium-ion batteries [J]. Nanoscale, 2012, 4(8): 2526−2542.

[3] ZUBI G, DUFO L R, PARDO N, PASAOGLU G. Concept development and techno-economic assessment for a solar home system using lithium-ion battery for developing regions to provide electricity for lighting and electronic devices [J]. Energy Conversion & Management, 2016, 122: 439−448.

[4] SCHIPPER F, AURBACH D. A brief review: Past, present and future of lithium ion batteries [J]. Russian Journal of Electrochemistry, 2016, 52(12): 1095−1121.

[5] YUAN Qing-feng, ZHAO Feng-gang, WANG Wei-dong, ZHAO Yan-ming, LIANG Zhi-yong, YAN Dan-lin. Overcharge failure investigation of lithium-ion batteries [J]. Electrochimica Acta, 2015, 178: 682−688.

[6] SHIM J H, LEE S, PARK S S. Effects of MgO coating on the structural and electrochemical characteristics of $LiCoO_2$ as cathode materials for lithium ion battery [J]. Chemistry of Materials, 2014, 26(8): 2537−2543.

[7] MUKAI K, SUGIYAMA J, IKEDO Y, AOKI Y, ANDREICA D, AMATO A. Structural and magnetic nature for fully delithiated Li_xNiO_2: Comparative study between chemically and electrochemically prepared samples [J]. Journal of Physical Chemistry C, 2010, 114(18): 8626−8632.

[8] LI Yan, LIU Kai-yu, LÜ Mei-yu, WEI Lai, ZHONG Jian-jian. Synthesis, characterization and electrochemical performance of AlF_3-coated $Li_{1.2}(Mn_{0.54}Ni_{0.16}Co_{0.08})O_2$ as cathode for Li-ion battery [J]. Transactions of Nonferrous Metals Society of China, 2014, 24(11): 3534−3540.

[9] RIM H, PARK H R, SONG M Y. Electrochemical performance of cobalt-substituted lithium nickel oxides synthesized from lithium and nickel carbonates and cobalt oxide [J]. Ceramics International, 2013, 39(2): 917−923.

[10] SEYMOUR I D, WALES D J, GREY C P. Preventing structural rearrangements on battery cycling: A first principles investigation of the effect of dopants on the migration barriers in layered $Li_{0.5}MnO_2$ [J]. Journal of Physical Chemistry C, 2016, 120(35): 19521−19530.

[11] PANG W K, LEE J Y, WEI Y S, WU S H. Preparation and characterization of Cr-doped $LiMnO_2$ cathode materials by Pechini's method for lithium ion batteries [J]. Materials Chemistry & Physics, 2013, 139(1): 241−246.

[12] JI Hong-mei, MIAO Xiao-wei, WANG Lu, QIAN Bing, YANG Gang. Effects of microwave-hydrothermal conditions on the purity and electrochemical performance of orthorhombic $LiMnO_2$ [J]. Acs Sustainable Chemistry & Engineering, 2013, 2(2): 359−366.

[13] DONG Tao, YU Xian-jin, ZHANG Li-peng, YANG Ping. Synthesis and properties of cathode materials $xLi_2MnO_3\cdot(1-x)LiMn_{1/3}Ni_{1/3}Co_{1/3}O_2$ for Li-ion batteries [J]. Journal of Nanoscience & Nanotechnology, 2014, 14(4): 3041−3045.

[14] NOH H J, YOUN S, CHONG S Y, SUN Y K. Comparison of the structural and electrochemical properties of layered $Li[Ni_xCo_yMn_z]O_2$ (x=1/3, 0.5, 0.6, 0.7, 0.8 and 0.85) cathode material for lithium-ion batteries [J]. Journal of Power Sources, 2013, 233: 121−130.

[15] PAN Cheng-chi, Zhu Yi-rong, YANG Ying-chang. HOU Hong-shuai, JING Ming-jun, SONG Wei-xin, YANG Xu-ming, JI Xiao-bo. Influences of transition metal on structural and electrochemical properties of $Li[Ni_xCo_yMn_z]O_2$ ($0.6\leq x\leq 0.8$) cathode materials for lithium-ion batteries [J]. Transactions of Nonferrous Metals Society of China, 2016, 26(5): 1396−1402.

[16] MARTHA S K, SCLAR H, FRAMOWITZ Z S, KOVACHEVA D, SALIYSKI N, GOFER Y, SHARON P, GOLIK E, MARKOVSKY B, AURBACH D. A comparative study of electrodes comprising nanometric and submicron particles of $LiNi_{0.50}Mn_{0.50}O_2$, $LiNi_{0.33}Mn_{0.33}Co_{0.33}O_2$, and $LiNi_{0.40}Mn_{0.40}Co_{0.20}O_2$ layered compounds [J]. Journal of Power Sources, 2009, 189(1): 248−255.

[17] HWANG S, KIM S M, BAK S M, KIM S Y, CHO B W, CHUNG K Y, LEE J Y, STACH E A, CHANG W. Using real-time electron microscopy to explore the effects of transition-metal composition on the local thermal stability in charged $Li_xNi_yMn_zCo_{1-y-z}O_2$ cathode materials [J]. Chemistry of Materials, 2015, 27(11): 3927−3935.

[18] DENG Long-zheng, WU Feng, GAO Xu-guang, LIU Zhen-tian, XIE Hai-ming. Synthesis and electrochemical properties of $LiNi_{0.87}Co_{0.10}Mg_{0.03}O_2$ cathode materials [J]. Transactions of Nonferrous Metals Society of China, 2015, 25(2): 527−532.

[19] CAO Hui, ZANG Yao, ZANG Jian, XIA Bao-jia. Synthesis and electrochemical characteristics of layered $LiNi_{0.6}Co_{0.2}Mn_{0.2}O_2$ cathode material for lithium ion batteries [J]. Solid State Ionics, 2005, 176(13−14): 1207−1211.

[20] Na Y K, YIM T, SONG J H, YU J S, LEE Z. Microstructural study on degradation mechanism of layered $LiNi_{0.6}Co_{0.2}Mn_{0.2}O_2$ cathode materials by analytical transmission electron microscopy [J]. Journal of Power Sources, 2016, 307: 641−648.

[21] XIANG Yan-hong, LI Jian, WU Xian-wen, LIU Zhi-xiong, XIONG Li-zhi, HE Ze-qiang, YIN Zhou-lan. Synthesis and electrochemical characterization of Mg-doped Li-rich Mn-based cathode material [J]. Ceramics International, 2016, 42(7): 8833−8838.

[22] WANG Ding, LI Xin-hai, WANG Zhi-xing, GUO Hua-jun, XU Yan, FAN Yu-lei, RU Juan-jian. Role of zirconium dopant on the structure and high voltage electrochemical performances of $LiNi_{0.5}Co_{0.2}Mn_{0.3}O_2$ cathode materials for lithium ion batteries [J]. Electrochimica Acta, 2015, 188: 48−56.

[23] SHI Yang, ZHANG Ming-hao, QIAN Dan-na, MENG Y S. Ultrathin Al_2O_3 coatings for improved cycling performance and thermal stability of $LiNi_{0.5}Co_{0.2}Mn_{0.3}O_2$ cathode material [J]. Electrochimica Acta, 2016, 203: 154−161.

[24] LIU Si-yang, ZHANG Cong-cong, SU Qi-li, LI Liang-yu, SU Jun-ming, HUANG Tao, CHEN Yan-bin, YU Ai-shui. Enhancing electrochemical performance of $LiNi_{0.6}Co_{0.2}Mn_{0.2}O_2$ by lithium-ion conductor surface modification [J]. Electrochimica Acta, 2016, 224: 171−177.

[25] NITHYA C, DEVI S B, GOPUKUMAR S. Role of Mg dopant on the electrochemical performance of $LiNi_{0.5}Co_{0.5}O_2$, cathode materials for lithium rechargeable batteries [J]. Journal of Materials Science, 2012, 47(19): 6784−6791.

[26] WANG Dan, HUANG Yan, HUO Zhen-qing, CHEN Li. Synthesize and electrochemical characterization of Mg-doped Li-rich layered $Li[Li_{0.2}Ni_{0.2}Mn_{0.6}]O_2$ cathode material [J]. Electrochimica Acta, 2013, 107(3): 461−466.

[27] ZHONG Sheng-kui, LIU Le-tong, LIU Jie-qun, WANG Jian, YANG Jian-wen. High-rate characteristic of F-substitution $Li_3V_2(PO_4)_3$ cathode materials for Li-ion-batteries [J]. Solid State Communications, 2009, 149(39−40): 1679−1683.

[28] LIAO Xiao-zhen, HE Yu-shi, MA Zi-feng, ZHANG Xiao-ming, WANG Liang. Effects of fluorine-substitution on the electrochemical behavior of $LiFePO_4$/C cathode materials [J]. Journal of Power Sources, 2007, 174(2): 720−725.

[29] YI Ting-feng, HAN Xiao, YANG Shuang-yuan, ZHU Yan-rong. Enhanced electrochemical performance of Li-rich low-Co $Li_{1.2}Mn_{0.56}Ni_{0.16}Co_{0.08-x}Al_xO_2$ ($0\leq x\leq 0.08$) as cathode materials [J]. Science China Materials, 2016, 59(8): 618−628.

[30] YU Hai-jun, ZHOU Hao-shen. High-energy cathode materials (Li_2MnO_3−$LiMO_2$) for lithium-ion batteries [J]. Journal of Physical Chemistry Letters, 2013, 4(8): 1268−1280.

[31] ZHANG Xi-hui, YU Chuang, HUANG Xiang-dong, ZHENG Jiang, GUAN Xiang-feng, LUO Dong, LI Li-ping. Novel composites $Li[Li_xNi_{0.34-x}Mn_{0.47}Co_{0.19}]O_2$ ($0.18\leq x\leq 0.21$): Synthesis and application as high-voltage cathode with improved electrochemical performance for lithium ion batteries [J]. Electrochimica Acta, 2012, 81: 233−238.

[32] WANG Jun, ZHANG Ming-hao, TANG Chang-lin, XIA Yong-gao, LIU Zhao-ping. Microwave-irradiation synthesis of $Li_{1.3}Ni_xCo_yMn_{1-x-y}O_2$ cathode materials for lithium ion batteries [J]. Electrochimica Acta, 2012, 80(1): 15−21.

[33] YU Chuang, LI Guang-she, GUAN Xiang-feng, ZHENG Jing, LI Li-ping. Composites $Li_{1+x}Mn_{0.5+0.5x}Ni_{0.5-0.5x}O_2$ ($0.1\leq x\leq 0.4$): Optimized preparation to yield an excellent cycling performance as cathode for lithium-ion batteries [J]. Electrochimica Acta, 2012, 61: 216−224.

[34] LIANG Long-wei, DU Ke, PENG Zhong-dong, CAO Yan-bing, DUAN Jian-guo, JIANG Jian-bing, HU Guo-rong. Co–precipitation synthesis of $Ni_{0.6}Co_{0.2}Mn_{0.2}(OH)_2$ precursor and characterization of $LiNi_{0.6}Co_{0.2}Mn_{0.2}O_2$ cathode material for secondary lithium batteries [J]. Electrochimica Acta, 2014, 130: 82−89.

[35] HUANG Zhen-jun, WANG Zhi-xing, ZHENG Xiao-bo, GUO Hua-jun, LI Xin-hai, JING Qun, YANG Zhi-hua. Structural and electrochemical properties of Mg-doped nickel based cathode materials $LiNi_{0.6}Co_{0.2}Mn_{0.2-x}Mg_xO_2$ for lithium ion batteries [J]. RSC Advances, 2015, 5(108): 88773−88779.

循环性能改善的 F−Mg 共改性 $LiNi_{0.6}Co_{0.2}Mn_{0.2-y}Mg_yO_{2-z}F_z$ 锂离子电池材料

陈启超，闫冠杰，罗利明，陈 飞，谢堂锋，戴世灿，袁明亮

中南大学 资源加工与生物工程学院，长沙 410083

摘 要：结合共沉淀法和球磨辅助下的高温固相法，合成层状氧化物正极材料 $Li[Ni_{0.6}Co_{0.2}Mn_{0.2-y}Mg_y]O_{2-z}F_z$ ($0\leq y\leq 0.12$, $0\leq z\leq 0.08$)，探究 F−Mg 掺杂对 $LiNi_{0.6}Co_{0.2}Mn_{0.2}O_2$ 材料的影响。与以往的研究相比，这种掺杂处理在首次库仑效率和循环性能方面的电化学性能得到实质改善。在充放电倍率为 0.2*C* 和电压范围为 2.8~4.4 V 的条件下，$Li[Ni_{0.6}Co_{0.2}Mn_{0.11}Mg_{0.09}]O_{1.96}F_{0.04}$ 的首次放电比容量和库伦效率分别为 189.7 mA·h/g 和 98.6%，100 次循环后容量保持率为 96.3%。电化学阻抗谱(EIS)结果表明，Mg−F 掺杂降低了电荷转移电阻，从而提高了反应动力学，这是材料具有更高倍率性能的主要原因。由于 $Li[Ni_{0.6}Co_{0.2}Mn_{0.11}Mg_{0.09}]O_{1.96}F_{0.04}$ 具有优异的电化学性能，被看作是很有前景的新型锂离子电池正极材料。

关键词：高镍正极材料；F−Mg 掺杂；高库伦效率；循环稳定性

(Edited by Xiang-qun LI)